J Mater Sci (2009) 44:4370–4378
DOI 10.1007/s10853-009-3655-9

Experimental and modeling study of the thermal conductivity of SiC_p/Al composites with bimodal size distribution

Ke Chu · Chengchang Jia · Xuebing Liang · Hui Chen · Hong Guo · Fazhang Yin · Xuanhui Qu

Received: 4 March 2009 / Accepted: 1 June 2009 / Published online: 16 June 2009

Abstract The thermal conductivity of SiC_p/Al composites with high volume fractions of 46 to 68% has been investigated. The composites were fabricated by pressureless infiltrating liquid aluminum into SiC preforms with monomodal and bimodal size distributions. The density measurement indicates that a small amount of pores is presented for the composites approaching their maximum volume fractions. An analytical model with an explicit expression is proposed for describing the thermal conductive behavior of the composites with multimodal-reinforced mixtures in terms of an effective medium approach taking into account the porosity effect. Predictions of the developed effective medium expression reveal good correspondence with the experimental results, and explore how each of the considered factors (i.e., particle size ratio, volume fraction ratio, and porosity) can have a significant effect on the thermal conductivity of the composites with bimodal mixtures.

Introduction

Particle-reinforced metal matrix composites with high reinforcement volume fractions are used for thermal management applications due to their excellent thermo-physical properties, tailorable thermal expansion, and low density [1–3]. In particular, Al matrix composites containing high volume fractions of SiC particles (SiC_p/Al) composites are receiving the most attention as potential candidates for a variety of use in advanced electronic packaging, and are currently competing with established materials such as Cu/W or Cu/Mo in the electronic packaging industry.

Monocrystalline SiC has a thermal conductivity around 500 W/mK which, although decreasing down to 270 W/mK in sintered polycrystalline material, is more than enough to be used as an electronic support. As for the matrix, the thermal conductivity of pure aluminum is about 237 W/mK, but it is dramatically reduced by elements in solid solution [4]. Since SiC features both excellent thermal properties of high thermal conductivity and concomitant low thermal expansion coefficients (CTEs), the volume fraction of embedded SiC particle as high as possible is required for microelectronic packaging. Composites being tested and produced by the industry usually incorporate reinforcements in amounts >60% [5]. Such high particle volume fraction can only be reached by using particle mixtures having bimodal size distributions. Although SiC particles having a bimodal size distribution are actually being used to produce high volume fraction SiC_p/Al composites, the numerical investigations on the thermal conductive behavior of such composites are rather limited [6]. To the best of our knowledge, a complete understanding of the influence of various factors on the thermal conductivity of the composites with bimodal mixtures is still missing. In order to assess the potential of and then tailor and optimize the properties of materials for specific applications, it is necessary to provide a numerical insight for the thermal conductive behavior of these composites.

K. Chu (✉) · C. Jia · X. Liang · H. Chen · X. Qu
School of Materials Science and Engineering, University of Science and Technology Beijing, Beijing 100083, China
e-mail: sinygm@yahoo.com.cn

H. Guo · F. Yin
Beijing General Research Institute for Nonferrous Metals, Beijing 100088, China

In previous reported studies [7, 8], high volume fraction composites composed of either monomodal or bimodal size distributions were produced by pressureless infiltration. This process consists of two steps: preparing SiC_p preforms by powder injection molding (PIM) and infiltrating aluminum alloys into preforms spontaneously through the capillary interaction that governs this infiltration process. An optimum aluminum alloy composition within the addition of Mg 4–8 wt%, Si 6–12 wt% is designed, in which there is no detrimental interfacial reaction products such as Al_4C_3 formed and the composites thus exhibit good thermo-mechanical properties. However, various degrees of pores can always appear as an unavoidable phase in composites during this process for many reasons. The porosity has no or little influence on CTE but may decrease strongly the thermal conductivity of a material [9, 10]. The quantitative characterization of its presence and influence on the thermal conductivity of the composites needs to be further investigated.

The purpose of this article is to study the thermal conductivity of SiC_p/Al composites obtained through pressureless infiltration of liquid aluminum alloy into SiC particles preforms having monomodal and, in particular, bimodal size distributions. The appearance of pores and their effect on the thermal conductivity of the composites are also treated. A theoretical model is proposed based on an effective medium approach for describing the thermal conductive behavior of multimodal-reinforced mixtures by considering the porosity effect. The model is then used to compare the experimental data and also exploits how each of the considered factors (i.e., particle size ratio, volume fraction ratio, and porosity) can have a significant effect on the thermal conductivity of the composites.

Experimental

Materials

Green α-SiC powders (99% pure) with different mean particle sizes of 14, 28, 40, and 80 μm were used as reinforcements in this study. The particles with 14 μm were used to produce composites with a monomodal size distribution. Three types of particle mixtures with different particle size ratios of 28/14, 40/14, and 80/14 μm were prepared for composites with a bimodal size distribution. The volume fraction ratio of coarse-to-fine particles were fixed to 3:2 for all bimodal mixtures, this is because the mixture having 60–67% of coarse particles can help the composites attain a maximum volume fraction [5, 11]. The chemical composition of the aluminum alloy for infiltration was Al–12 wt%Si–8 wt%Mg.

Fabrication of preforms

The SiC_p preforms were prepared by PIM using wax-based binder. The binder composition was 65 wt% PW (paraffin wax) + 29 wt% HDPE (high density polythene) + 1 wt% SA (stearic acid). The feedstocks for PIM were produced by mixing SiC powder and the binder with a SiC_p loadage (namely particle volume fraction for final composites) range of 55 to 68 vol.% in the double planetary mixer at a temperature of 150 °C. The dense cylindrical samples with a dimension of 40 mm in diameter and 5 mm in height were then prepared by PIM at an injection temperature of 150 °C and an injection pressure of 80 MPa [7]. The injection samples were made to porous performs in a two-step procedure: solvent debinding in gasoline for 28 h (for removing the most of binders), and then thermal debinding-pre-sintering (for removing the residue binders and achieving the preforms with opening pores and enough strength) in hydrogen atmosphere under specified processing conditions. Figure 1 shows the process of thermal debinding-pre-sintering.

Fabrication of composites

The pressureless infiltration of liquid Al alloy into SiC preforms was carried out in a horizontal tube furnace provided with end-cap fittings to control the process atmosphere. After SiC preforms soaked above liquid Al alloy at 950 °C for 2 h, the specimens were cooled down within furnace to room temperature. The composite plates could be obtained after getting rid of the remained aluminum left on the surface of the composites. The characteristics of the samples were shown in Table 1.

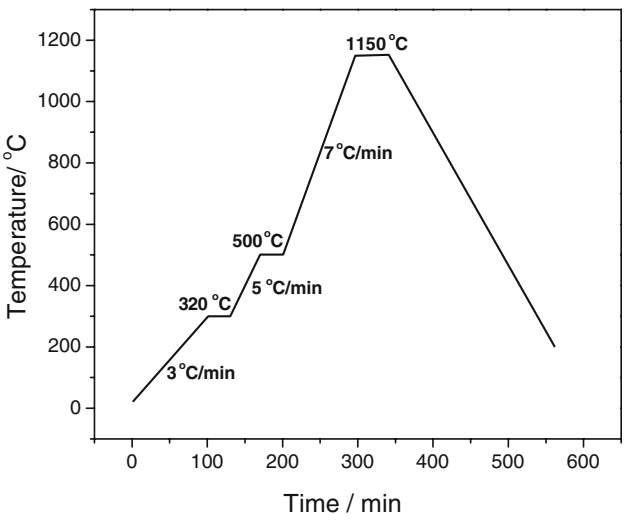

Fig. 1 Process of thermal debinding-pre-sintering

Table 1 The characteristics of all the samples investigated in this study

Particle size distribution (μm)		V_p (%)	ξ (%)	K_c (W m^{-1} K^{-1})	σ_c (10^6 Ω^{-1} m^{-1})
Monomodal	14	46	<1	156	7.33
		50	<1	163	6.98
		53	5.3	145	–
Bimodal	28/14	57	<1	170	5.09
		59	1.2	169	–
		63	3.7	160	–
	40/14	59	<1	178	4.32
		63	<1	183	3.85
		65	4.4	158	–
	80/14	63	<1	184	3.58
		65	<1	186	3.43
		68	<2.3	176	–

V_p is the particle volume fraction, ξ is the porosity, K_c and σ_c are the thermal conductivity and electronic conductivity of the composites, respectively

Electronic conductivity measurement

The room temperature static electric conductivity was measured with the four probe method for determining the matrix thermal conductivity. Only pore-free samples (porosity <1%) were considered in order to eliminate the influence of porosity. All specimens had a rectangular cross section Q of 1 × 1 mm^2 and 25 mm length. Both ends of the specimens were connected to a constant current source, which provided a current of magnitude I. The potential drop V was measured over the distance L with the aid of two knife-edge ridges pressed on the sample. The conductivity $\sigma = (I/V)(L/Q)$ was calculated by taking the mean value of two voltage and current measurements for normal and reversed current direction in order to minimize the effect of contact voltages.

Thermal conductivity measurement

The laser flash method was used to measure the thermal diffusivity of the composites at room temperature. The thermal diffusivity measurement was performed on a JR-3 thermo-physical testing instrument, which involves exposing the front face of the sample to a short laser burst and recording the temperature rise on the rear face. The uncertainty in the thermal measurements is ±2%. The density of the composites was measured by Archimedes' principle. The porosity was estimated by calculating the difference between the theoretical and the actual composite density. The specific heat was derived from the theoretical value calculated by the rule of mixture. The thermal conductivity of the composites was then calculated as a product of the density, thermal diffusivity, and specific heat. All measurement results are also shown in Table 1.

Experimental results and discussion

Permeability of the preforms

It can be found in Table 1 that electronic packaging with particle volume fractions >60% can be easily achieved using particles with bimodal mixtures in this study. The larger the size ratio of particle mixtures, the higher the volume fraction. The mixtures with a size ratio of 80/14 μm having 60% of coarse particles show the maximum volume fraction of 0.68, a value of 28% higher than those obtained for performs containing a single particle size of 14 μm. Nevertheless, a small amount of pores can also been found in both composites with monomodal and bimodal size distributions. In general, pores can arise from the poor wettability of the ceramic by the metals or the evaporation of magnesium under high temperature. Differential shrinkage due to the different CTEs of the aluminum and SiC also aids the formation of microspores [8, 12]. However, for the same infiltrating condition, the selective appearance of pores for all fabricated composites demonstrates that this is related to the other parameters such as particle volume fraction and particle size.

Data in Table 1 reveal that the porosity becomes notable when particles' content approaches their maximum compactness. Martins et al. [13] examined a capillary-bundle model for describing the infiltration kinetics of liquid metal into a porous preform. The infiltration rate of the liquid metal is characterized by a parameter Φ:

$$\Phi = \frac{r_c \gamma_{LV} \cos\theta}{2\mu}, \tag{1}$$

where γ_{LV} the surface tension, r_c the capillary radius, and μ the viscosity of the liquid. Equation 1 reveals that the Φ increases with r_c, indicating that preforms with larger capillary radius have a higher infiltration rate.

Carman [14] proposed another parameter called hydraulic radius (r_h), which is related to the mean particle size (d) and particle compactness of preforms (namely volume fraction, V_p), given by:

$$r_h = \frac{r_c}{2} = \frac{(1 - V_P)d}{6V_p}. \tag{2}$$

From Eq. 2, one can realize that the increase in V_p and a decrease in d can make a decline in the value of r_h, hence retard infiltration of molten Al into the voids. The change of r_h with V_p and d for the performs made of single particles can be directly calculated by means of the above model. However, in the present cases, most of preforms are

packed as bimodal mixtures, using Eq. 2 requires that one chooses a uniform diameter reflecting the mixtures of different particle diameters firstly. A way of tackling this problem is to define a characteristic particle size representing the mean diameter of reinforced mixtures through the overall specific surface area of the preform. The specific surface area (I) for preforms with single size particles can be defined as a product of the surface area of one particle (πd^2) and the total number of the particles ($6V_p/\pi d^3$) at a given volume fraction (V_p), which gives

$$I = \frac{6V_P}{d}. \tag{3}$$

For bimodal mixtures with two distinct sizes (d_1 and d_2), specific surface area then becomes:

$$I = \frac{6V_1}{d_1} + \frac{6V_2}{d_2}, \tag{4}$$

where V_1 and V_2 are the actual fraction of sizes d_1 and d_2 particles in the composites, respectively ($V_1 + V_2 = V_p$). Since Eqs. 3 and 4 are equivalent, the characteristic diameter (D) for bimodal mixtures can be calculated as follows:

$$D = \frac{V_P d_1 d_2}{V_1 d_2 + V_2 d_1}. \tag{5}$$

Figure 2 shows the hydraulic radius (r_h) as a function of particle volume fraction (V_p) for different preforms with monomodal and bimodal distributions using Eqs. 2 and 5. With the combination of the data in Table 1, the critical hydraulic radius needed for full infiltration accounting for the present samples can be determined as 2.3 μm, and thus the hydraulic radii below this critical value can lengthen the time needed for an equal amount of infiltration, which leads to the consequence that the preforms are incompletely infiltrated, leaving behind the various degrees of micro-pores. Therefore, the presence of pores in the composites with maximum volume fraction of particles arises from their rather small hydraulic radii, which are lower than critical r_h. The good fitting results between the theoretical analysis and experimental measurements also support Carmon's model incorporated into bimodal effect and indicate that it is sufficiently accurate to give a guideline for the permeability of preforms with prescribed size distributions.

Thermal conductivity

Figure 3 shows the measured thermal conductivity of SiC_p/Al samples with monomodal and bimodal particle size distributions. It can be found that this value is proportional to the particle volume fraction confirming that the SiC_p has a higher thermal conductivity than the

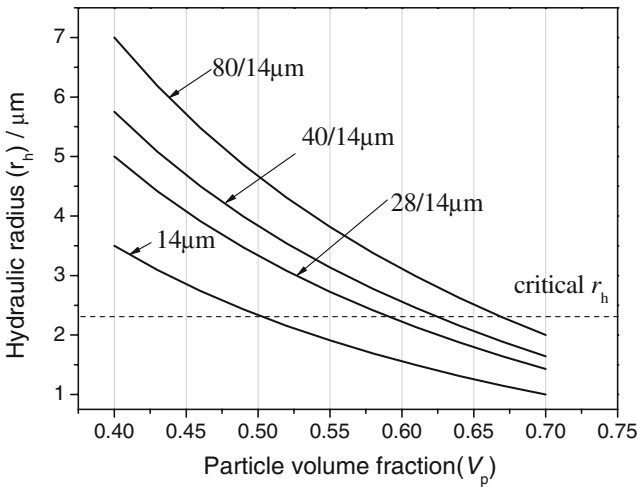

Fig. 2 Hydraulic radius for pressureless infiltration of liquid metals into monomodal and bimodal particle preforms versus particle volume fraction obtained from Eqs. 2 and 5. *Dash line* stands for the critical hydraulic radius determined from the experimental data in Table 1

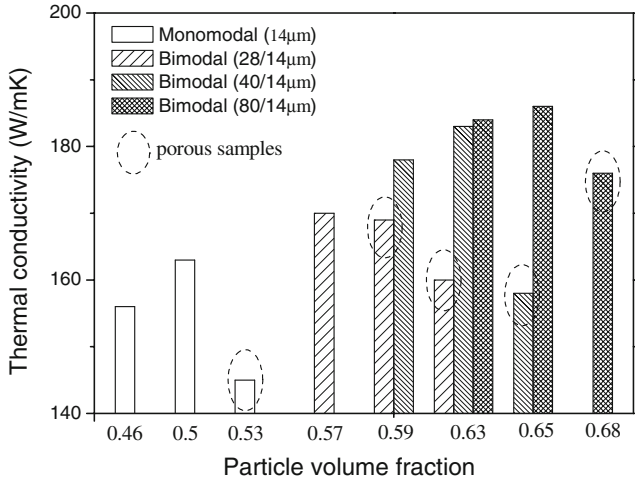

Fig. 3 Dependence of experimentally determined thermal conductivity on the particle volume fraction for pressureless infiltrated SiC_p/Al composites with monomodal and bimodal particle size distributions

matrix. A particles' selection of bimodal mixtures, implying the increase in the amount of particles content, provides the pronounced improvement in the overall conductivity. For the reinforced mixtures system containing the fine particles with fixed particle size, incorporating the larger coarse particles, corresponding to rise in size ratio, not only heightens the volume fraction, but also deceases the value of interfacial thermal resistance (ITR) that arises from the significant diffuse scattering of phonons in both the matrix and the particles when the heat-carriers (electrons and phonons) propagate across the interfaces [15]. Therefore, the composites conductivity

can be further enhanced, as shown in Fig. 3 the composites with bimodal mixtures of larger size ratio exhibit the higher conductivity than those obtained by bimodal mixtures of smaller one at the same volume fraction. However, the above "clean" rules derived from the experiments are marred more or less by the presence of a certain amount of porosity, which can impair the composites thermal conductivity due to scattering the heat flow.

Numerical analyses

For the prediction of the thermal conductivity of the composites with a bimodal or multimodal size distribution, Molina et al. [6] recently proposed a model based on a differential effective medium scheme. The application of this approach is somewhat cumbersome, because it yields an implicit relationship or integral description of the effective conductivity of the composites, and it needs to be solved numerically. In the following, a mathematically simpler model with an explicit expression in terms of an effective medium approximation (EMA) is developed and discussed for quantitatively describing the thermal conductivity of composites with multimodal mixtures and porosity content.

Modeling

Hasselman and Johnson [16] extended the classical study of Maxwell [17] to consider simply spherical particulate and cylindrical fiber-reinforced matrix composites and derived a Maxwell-Garnett type EMA for calculating composites thermal conductivity in which the Kapitza ITR [18] effect and particle size are included. Here we extend their theory to a multimodal size distribution.

We consider a cluster of particles with thermal conductivity K_p embedded in an effective matrix with thermal conductivity K_m. The cluster of particles, enclosed by a spherical region of radius R, consists of n spherical particles of radius a. Assuming negligible interaction between the particles, the temperature T_p within the dispersed particles and the temperature T_m in the surrounding matrix are assumed to have the following form [16]:

$$T_p = rA\cos\theta, \tag{6a}$$

$$T_m = (\nabla T)r\cos\theta + \frac{nB}{r^2}\cos\theta, \tag{6b}$$

where (∇T) is the temperature gradient at a radial distance r ($r \gg R$) from the center of the spherical cluster region R; θ is the angle between the radius vector $\bar{r}$ and the temperature gradient; the unknown constants of A and B needs to be solved. Equation 6 satisfies the following boundary conditions at $r = a$:

$$K_p\frac{\partial T_p}{\partial \bar{r}} = K_m\frac{\partial T_m}{\partial \bar{r}}, \tag{7a}$$

$$T_p - T_m = -\left(\frac{K_p}{h}\right)\frac{\partial T_p}{\partial \bar{r}}, \tag{7b}$$

where h is the Kapitza conductance between the spherical dispersions and the matrix.

The constants A, B in Eq. 6 can be solved by Eq. 7 and yield:

$$A = (\nabla T)\left(\frac{3}{2K_p/ah + K_p/K_m + 2}\right), \tag{8a}$$

$$B = (\nabla T)\left(\frac{K_p/ah - K_p/K_m + 1}{2K_p/ah + K_p/K_m + 2}\right)a^3. \tag{8b}$$

Since the particle volume fraction V_p can be defined as $V_p = n(a/R)^3$, after substituting the solved B from Eq. 8b, Eq. 6b can be re-written as:

$$T_m = (\nabla T)\left[r + V_p R^3\left(\frac{K_p/ah - K_p/K_m + 1}{2K_p/ah + K_p/K_m + 2}\right)\frac{1}{r^2}\right]\cos\theta. \tag{9}$$

Equation 9 can be extended to multiple reinforcement phases (i), each of which corresponds to a cluster of particles composed of n spherical particles of a given particles of radius a_i having volume fraction of V_{p_i}. In such a scheme the T_m depends on the cumulative effect of N size classes of reinforcements within a region R, which becomes:

$$T_m = (\nabla T)\left\{r + R^3\sum_i^N\left[V_{p_i}\left(\frac{K_p/a_ih - K_p/K_m + 1}{2K_p/a_ih + K_p/K_m + 2}\right)\right]\frac{1}{r^2}\right\}\cos\theta. \tag{10}$$

Now if all these clusters of particles are treated as an "effective homogeneous medium" of radius R and thermal conductivity K_c, suspended in a matrix of conductivity K_m, the T_m at any radial location r ($r \gg R$) is given as

$$T_m = (\nabla T)\left[r + R^3\left(\frac{K_m - K_c}{2K_m + K_c}\right)\frac{1}{r^2}\right]\cos\theta. \tag{11}$$

Since the two expressions, Eqs. 10 and 11 are equivalent, it follows that

$$\sum_i^N\left[V_{p_i}\left(\frac{K_p/a_ih - K_p/K_m + 1}{2K_p/a_ih + K_p/K_m + 2}\right)\right] = \frac{K_m - K_c}{2K_m + K_c}. \tag{12}$$

For explicit expression of K_c, Eq. 12 can be rearranged as:

$$K_c = K_m\left(\frac{1 + 2A}{1 - A}\right) \tag{13a}$$

with

$$A = \sum_{i}^{N} \left[V_{p_i} \left(\frac{K_{p_i}^{eff}/K_m - 1}{K_{p_i}^{eff}/K_m + 2} \right) \right], \tag{13b}$$

$$K_{p_i}^{eff} = \frac{K_p}{1 + K_p/a_i h}, \tag{13c}$$

where K_p^{eff} stands for the effective thermal conductivity of the particles due to the existing of the interface thermal conductance between the two solid phases. The volume fractions of mixed particles of N size classes fulfill the relationship: $V_p = \sum_{i}^{N} V_{p_i}$.

Equation 13 gives an explicit relationship for the effective conductivity of the composites with a prescribed size distribution. Typically, for the composites with uniformly distributed particles of single size, Eq. 13 reduces to

$$K_c = K_m \left[\frac{1 + 2V_p \left(\frac{K_p^{eff}/K_m - 1}{K_p^{eff}/K_m + 2} \right)}{1 - V_p \left(\frac{K_p^{eff}/K_m - 1}{K_p^{eff}/K_m + 2} \right)} \right]. \tag{14}$$

Equation 14 is identical to Hasselman and Johnson's model [16] and Benveniste's [19] self-consistent scheme.

To quantitatively account for the composites of ternary system consisting of metal matrix, ceramic particles, and pores, we can apply a double EMA, where we consider the particles to be embedded in a so-called "effective matrix" made up of a composite of matrix with certain amount of pores (namely porous matrix). The effective fraction of pores ξ' in the effective matrix is defined as:

$$\xi' = \frac{\xi}{1 - V_p}. \tag{15}$$

The effective matrix thermal conductivity K_m^{eff}, derived from Eq. 14 by assuming $K_p = 0$ is

$$K_m^{eff} = \frac{K_m(1 - \xi')}{1 + 0.5\xi'}. \tag{16}$$

The thermal conductivity of the overall composite is obtained in terms of the effective matrix conductivity and embedded particles, by replacing K_m in Eq. 13 with K_m^{eff}, which takes the following form:

$$K_c = K_m^{eff} \left(\frac{1 + 2A}{1 - A} \right), \tag{17a}$$

where

$$A = \sum_{i}^{N} \left[V_{p_i} \left(\frac{K_{p_i}^{eff}/K_m^{eff} - 1}{K_{p_i}^{eff}/K_m^{eff} + 2} \right) \right], \tag{17b}$$

$$K_{p_i}^{eff} = \frac{K_p}{1 + K_p/a_i h}. \tag{17c}$$

Equation 17 is the general EMA formulation that contains all the effects of conductivity of the individual phases (K_m, K_p), particle size, size distribution, volume fraction, ITR, and additional microstructural parameter of porosity on K_c for the particulate composites. From Eq. 17, the K_c can be easily solved for the composites with multimodal mixtures and a given porosity.

Determination of material parameters

In Eq. 17, the accurate values of materials parameters (K_m, h, K_p) are needed for calculations. However, according to the reported data [5, 6, 8, 10, 20], these parameters cover wide ranges depending on the purity of the particles, as well as the fabrication route, thus it is very important to determine their pertinent values accounting for the present materials. Alternatively, K_m can be derived from the electrical conductivity measurements (see Refs. [6, 10] for more details), a value of 150 W/mK is obtained in the present case. The value of the intrinsic interfacial thermal conductance, h, can be estimated by a simple Debye model in terms of the acoustic mismatch theory [18], and calculated to be 6.68×10^7 W/m^2/K (see Ref. [19] for more details). We then take into account all the pore-free composites with monomodal size distribution, and substitute two sets of data for K_c (Table 1), and related other parameters of K_m, d, and V_p into H–J model (Eq. 14), the average K_p value of 246 W/m/K and can be ultimately back-calculated.

Numerical results and comparison with experiments

Figure 4 shows the predictions obtained by the present model for the thermal conductivity of pore-free SiC_p/Al composites (K_c) versus particle size ratio of coarse-to-fine particles (δ_{cf}, fix d_f) with different given sizes of fine particles (d_f) at fixed particle volume fraction, $V_p = 0.6$, containing 60% of coarse particles. An increase in d_f implies a decrease in the average ITR of the whole composite, resulting in an obvious enhancement in K_c. Considering the variations of δ_{cf} in the mixtures system, the K_c of composites with a small d_f increases significantly with δ_{cf} as $\delta_{cf} < 8$, then very slightly increases and gradually remains to be a constant with δ_{cf} as $\delta_{cf} > 8$. When $\delta_{cf} < 8$, the δ_{cf} has a marked effect on K_c at small d_f (e.g., $d_f < 14$ μm), whereas at large d_f (e.g., $d_f > 40$ μm), the K_c hardly changes no matter what the value of δ_{cf} is.

Figure 5 shows the predictions for the K_c of pore-free composites versus δ_{cf} (fix $d_f = 14$ μm) with different contents of coarse particles in the mixture (V_{cp}) at fixed particle volume fraction, $V_p = 0.6$. The significant increase in K_c with V_{cp} is attributed to the reduction of the average ITR. As clearly can be seen, the effect of δ_{cf} on K_c also

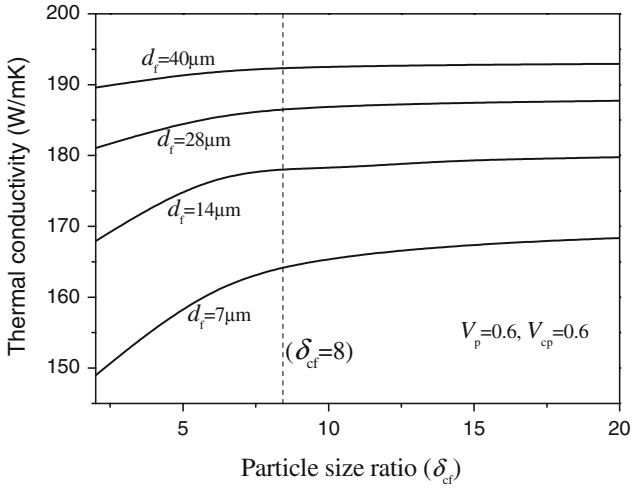

Fig. 4 Dependence of predicted thermal conductivity of dense SiC_p/Al composites (K_c) on the particle size ratio of coarse-to-fine particles (δ_{cf}, fix d_f) for bimodal mixtures with different given sizes of fine particles (d_f) at fixed particle volume fraction of $V_p = 0.6$, having 60% of coarse particles ($V_{cp} = 0.6$)

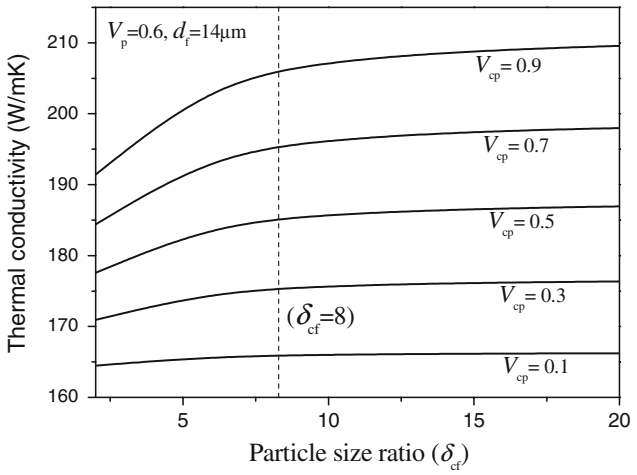

Fig. 5 The predicted thermal conductivity of dense composites (K_c) as a function of particle size ratio (δ_{cf}, fix $d_f = 14$ μm) for bimodal mixtures with different contents of coarse particles in the mixture (V_{cp}) at fixed particle volume fraction of $V_p = 0.6$

depends on the value of V_{cp} that the increase in V_{cp} results in an increasingly pronounced enhancement in K_c with δ_{cf} as $\delta_{cf} < 8$.

These prediction results suggest that, for composites with bimodal mixtures, the K_c shows a remarkable increase with particle size (either d_f or d_c) and V_{cp} at a given volume fraction due to the decease in ITR. The notable effect of δ_{cf} on K_c depends on the values of d_f, V_{cp}, and δ_{cf} itself, all of which should lie within the ranges of $d_f < 14$, $V_{cp} > 0.3$, and $\delta_{cf} < 8$, respectively. Once beyond either of these ranges, K_c varies slightly with δ_{cf}, especially at $d_f > 40$, or $V_{cp} < 0.1$, or $\delta_{cf} > 8$, the effect of δ_{cf} on K_c is negligible, as more clearly illustrated in Fig. 6a–c for the total range of particle volume fraction. Here we only perform the numerical analysis for the limit case of present composites. It is worth noting that the similar variation of K_c for other particulate composite system with bimodal mixtures depending on the parameters of d_f, V_{cp}, and δ_{cf} is still existed, but the critical ranges of these values are changed. One can use Eq. 17 to determine the pertinent ranges of d_f, V_{cp}, and δ_{cf} for any particulate composite.

Figure 7 shows the dependence of the predicted thermal conductivity of the composites on the porosity for the porous composites with monomodal and bimodal size distributions. It can be clearly seen that the effect of porosity on K_c only depends on the thermal conductivity of the pore-free composites no matter whether the particle distribution is monomodal or bimodal, and makes nearly the same linear decrease in K_c for all the samples at a given porosity. For the considered porosity of 6.3%, the thermal conductivity decrement is about 10.2%, a value of 60% higher than its corresponding porosity, demonstrating that porosity has a significant impact on the composites thermal conductivity.

These final values calculated with the present model, taking into account all the effects of particle size dependent of ITR, particle size, size distribution, and porosity are compared with experimental results, as shown in Fig. 8. It is obvious that the calculated values provide a satisfactory agreement to experimental data.

From the above experimental results and numerical analyses, we learn that using larger coarse particles with suitably fine particles accommodating into the free space left by coarse particles can greatly improve the composites thermal conductivity by both upgrading the particle volume fraction and weakening the effect of ITR. However, larger particles also increase the possibility of particle fracture during processing and performance [21]. Therefore, taking both these effects into consideration for the design of SiC_p/Al composites with the desired thermal and mechanical properties are of great importance.

Conclusions

SiC_p/Al composites with monomodal and bimodal size distributions having particle volume fractions from 46 to 68% were prepared by pressureless infiltration and characterized with respect to their thermal conductivity. The composites with bimodal mixtures with substantially large particle size ratio can reach higher particle volume fraction and the higher thermal conductivity compared with those of single-sized particles. Various degrees of porosity can present in composites when the particles contents approach their maximum volume fractions due to the shortage of full

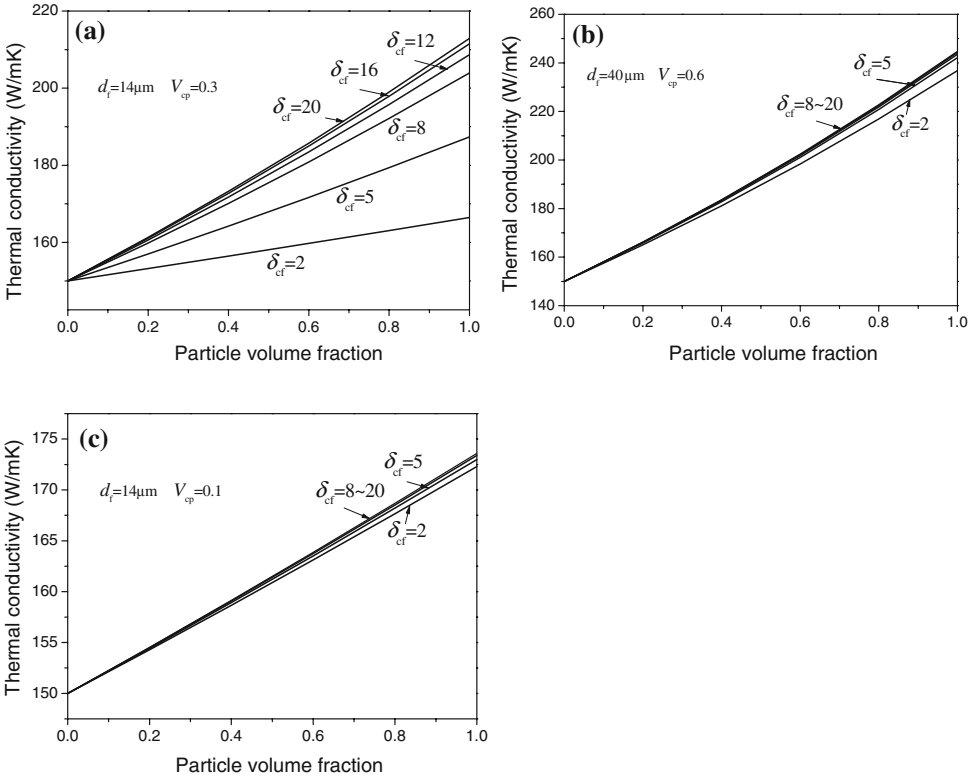

Fig. 6 The predictions for the effect of particle size ratio (δ_{cf}) on the thermal conductivity of dense composites (K_c) over the total range of particle volume fraction (V_p): **a** The K_c versus V_p with different δ_{cf}, where the fine particle size, $d_f = 14$ μm, and the coarse particles content in the mixtures, $V_{cp} = 0.3$. The δ_{cf} shows marked effect on K_c as $\delta_{cf} < 8$; **b** The K_c versus V_p with different δ_{cf}, where $d_f = 40$ μm, $V_{cp} = 0.6$. The effect of δ_{cf} is negligible; **c** The K_c versus V_p with different δ_{cf}, where $d_f = 14$ μm, $V_{cp} = 0.1$. The effect of δ_{cf} is negligible

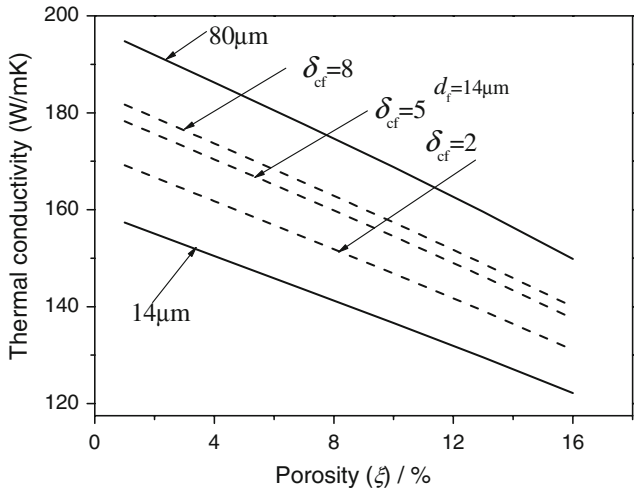

Fig. 7 The predicted thermal conductivity of the composites (K_c) as a function of porosity (ξ) for the composites with monomodal (14, 80 μm) and bimodal size distributions ($\delta_{cf} = 2$, $\delta_{cf} = 5$, $\delta_{cf} = 8$, all with fixed $d_f = 14$ μm)

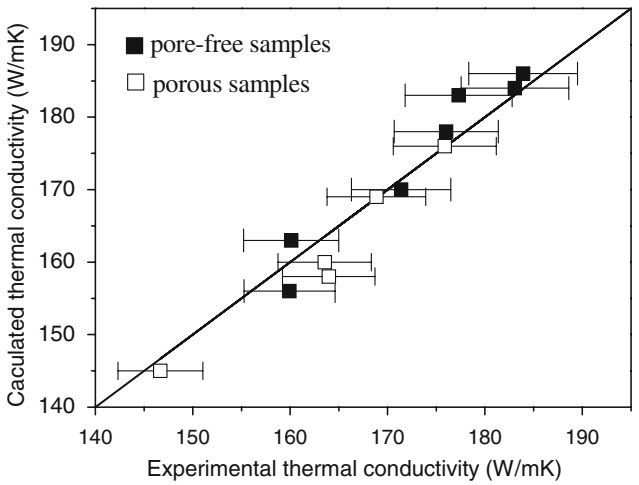

Fig. 8 Comparison of the thermal conductivity calculated with the developed effective medium model and that determined experimentally for samples in Table 1, the measured uncertainty is ±2%. *Filled squares* correspond to pore-free (porosity <1%) samples, whereas *opened squares* correspond to samples with a given porosity content. The *line* represents the identity function, showing the good agreement between the predictions and the measured values

infiltration caused by their rather small hydraulic radii, which are lower than the critical hydraulic radius.

Experimental results are compared to a developed analytical model derived from the EMA theory, and are shown to agree well with predictions for the composites with various size distributions and porosity contents. Numerical results based on the present model indicate that the composites thermal conductivity shows a marked increase with increasing particle size and coarse particles content, but a significant decrease with the increase in porosity. The notable effect of particle size ratio (δ_{cf}) on composites conductivity depends on the values of itself, fine particle size (d_f), coarse particles content (V_{cp}), and all of which,

for the present composites, should roughly lie within the ranges of $d_f < 14$ μm, $V_{cp} > 0.3$, and $\delta_{cf} < 8$, respectively.

Acknowledgements This study is financially supported by National 863 Plan Project of China (No. 2008AA03Z505). The authors would like to thank Prof. H. Guo, from Beijing Research Institute of Non-ferrous Metals, for the supply of SiC powders and performing the pressureless infiltrations.

References

1. Byung GM, Dong SL, Park SD (2001) Mater Chem Phys 72:42
2. Robins M (2000) Electron Packag Prod 40:50
3. Huber T, Degischer HP, Lefrance G, Schmitt T (2006) Compos Sci Technol 66:2206
4. Arpón R, Molina JM, Saravanan RA, García CC, Louis E, Narciso J (2003) Acta Mater 5:3145
5. Molina JM, Piñero E, Narciso J, García CC, Louis E (2005) Curr Opin Solid State Mater Sci 9:202
6. Molina JM, Narciso J, Weber L, Mortensen A, Louis E (2008) Mater Sci Eng A 480:483
7. Ren SB, He XB, Qu XH (2007) Powder Metall 50(3):255
8. Ren SB, He XB, Qu XH, Humail IS, Li Y (2007) Compos Sci Technol 67:2013
9. Shen YL (1997) Mater Sci Eng A 237:102
10. Molina JM, Prieto R, Narciso J, Louis E (2009) Scr Mater 60:582
11. Molina JM, Saravanan RA, Arpón R, García CC, Louis E, Narciso J (2002) Acta Mater 50:247
12. Zhang L, Qu XH, He XB, Duan BH, Ren SB, Qin ML (2008) Mater Sci Eng A 489:285
13. Martins GP, Olson DL, Edwards GR (1998) Metall Trans B 19:95
14. Carman PC (1941) Soil Sci 52:1
15. Majumdar A, Reddy P (2004) Appl Phys Lett 84:4768
16. Hasselman DPH, Johnson LF (1987) J Compos Mater 21:508
17. Maxwell JC (1904) A treatise on electricity and magnetism. Oxford University Press, Oxford
18. Swartz ET, Pohl RO (1989) Rev Mod Phys 61:605
19. Benveniste Y (1987) J Appl Phys 61:2840
20. Chu K, Jia CC, Liang XB, Chen H, Guo H (2009) J Mater Des 30:3497
21. Mummery PM, Derby B, Scruby CB (1993) Acta Metall Mater 41:1431